Usefulness of the Apparent Diffusion Coefficient in Line Scan Diffusion-Weighted Imaging for Distinguishing between Squamous Cell Carcinomas and Malignant Lymphomas of the Head and Neck

Masayuki Maeda, Hiroya Kato, Hajime Sakuma, Stephan E. Maier, and Kan Takeda

BACKGROUND AND PURPOSE: **Squamous cell carcinoma (SCC) and lymphoma are common malignant tumors of the head and neck. The purpose of this study was to determine whether the apparent diffusion coefficient (ADC) in line scan diffusion-weighted imaging (LSDWI) is useful for distinguishing between SCC and lymphoma of the head and neck.**

METHODS: **LSDWI was prospectively performed in 39 patients with SCC and in 14 patients with lymphoma. Images were obtained with a diffusion-weighted factor (*b* factor) of 5 and 1000 s/mm^2, and ADC maps were generated. ADC values were measured for the two types of tumor.**

RESULTS: **Mean ADC values were $0.96 \pm 0.11 \times 10^{-3}$ mm^2/s for SCC and $0.65 \pm 0.09 \times 10^{-3}$ mm^2/s for lymphoma; the difference was significant ($P < .001$). All but one of the patients with lymphoma had ADC values lower than the lowest ADC (0.76×10^{-3} mm^2/s) in patients with SCC. When an ADC of 0.76×10^{-3} mm^2/s was used to distinguish between SCC and lymphoma, accuracy was 98% (52 of 53 lesions).**

CONCLUSION: **ADC values appear to be useful for distinguishing between SCC and lymphoma in the head and neck.**

Diffusion-weighted (DW) imaging is a technique for evaluating the rate of microscopic water diffusion in tissues. Since the introduction of the echo-planar technique, DW imaging has been successfully used to evaluate diseases of the CNS, particularly in the diagnosis and management of cerebral ischemia (1–4). DW imaging has been applied to CNS tumors. The results of comparisons of the apparent diffusion coefficient (ADC) and histopathologic findings have strongly suggested that greater cellularity is associated with more restricted diffusion (5, 6).

DW imaging is potentially useful in the evaluation of head and neck lesions (7–10), and ADC measurements have suggested that this imaging method may be useful for their characterization (7). Although results of initial studies were both challenging and promising, one drawback was the technical difficulty in assessing diffusion by echo-planar DW imaging. Because echo-planar DW imaging is limited by notable susceptibility artifacts in the head and neck due to the presence of dental work, as well as adjacent air and bone, it may be difficult to obtain precise ADC measurements in lesions located here. Therefore, DW imaging techniques that are insensitive to susceptibility artifacts appear to be necessary for the evaluation of head and neck lesions. We propose the application of line scan DW imaging (LSDWI) in the head and neck because this technique is inherently insensitive to susceptibility artifacts (11–14).

Squamous cell carcinoma (SCC) is the most common malignant tumor of the head and neck, but lymphoma is also common in this region. Conventional MR imaging findings are often nonspecific for SCC versus lymphoma (15, 16). The objective of this study was to evaluate the usefulness of the ADC value in LSDWI for distinguishing between SCC and lymphoma of the head and neck.

Methods

Patients

A total of 154 consecutive patients underwent clinical MR imaging over a 20-month period at a university hospital for the

Received May 26, 2004; accepted after revision September 17.

From the Departments of Radiology (M.M., H.S., K.T.) and Pathology (H.K.), Mie University School of Medicine, Japan, and the Department of Radiology (S.E.M.), Brigham and Women's Hospital, Boston, MA.

Address reprint requests to Masayuki Maeda, MD, Department of Radiology, Mie University School of Medicine, 2–174 Edobashi, Tsu, Mie 514-8507, Japan.

TABLE 1: Locations of SCCs and lymphomas

Lesion	Locations
SCC (n = 39)	Nasopharynx (n = 2), oropharynx (n = 9), hypopharynx (n = 13), paranasal sinuses and nasal cavity (n = 7), oral cavity (n = 4), larynx (n = 2), external auditory canal (n = 1), lacrimal sac (n = 1)
Lymphoma (n = 14)	Deep cervical spaces (n = 4), nasopharynx (n = 1), paranasal sinuses and nasal cavity (n = 4), oral cavity (n = 1), external auditory canal (n = 2), orbit (n = 2)

evaluation of head and neck tumors. The following patients were excluded from the study: (1) 30 patients in whom a pathologic diagnosis of the tumor was not obtained; (2) 42 patients in whom pathologic examination of the tumor showed a tumor type other than SCC or lymphoma; (3) 11 patients who received radiation therapy, chemotherapy, or both before MR study; and (4) 13 patients with tumors that were <10 mm in minimal transverse diameter on MR images or difficult to detect on T2-weighted images. In addition, five patients who met the inclusion criteria were excluded because their images showed motion artifacts. Consequently, we included 53 patients (39 with SCC and 14 with lymphoma). Patients with SCC included eight women and 31 men (age range, 41–84 years; mean age, 64.6 years), and those with lymphoma included seven women and seven men (age range, 7–86 years; mean age, 57.3 years). Table 1 shows the locations of their SCCs and lymphomas.

In all patients, the final diagnosis was based on pathologic findings in biopsy specimens. Biopsy was usually performed by means of fiberscopic guidance or endoscopic sinus surgery. In orbital lesions or those in the deep cervical spaces, open biopsy was performed. SCCs were classified as well differentiated (n = 8), moderately differentiated (n = 27), or poorly differentiated (n = 4). Lymphomas were classified as diffuse large B-cell lymphoma (n = 5), marginal zone B-cell lymphoma (n = 4), natural killer–cell/T-cell lymphoma (n = 3), Hodgkin lymphoma (mixed cellularity, n = 1), or follicular lymphoma (n = 1).

The mean maximum diameters of the tumors on MR images were 36.2 ± 12.9 mm (range, 20–60 mm) for SCCs and 37.1 ± 16.7 mm (range, 20–70 mm) for lymphomas.

MR Imaging Sequences

MR imaging was performed by using a 1.5-T MR imaging system (Signa, GE Medical Systems, Milwaukee, WI). A neurovascular array coil was used to allow coverage from the skull base to the thoracic inlet. All patients underwent conventional MR imaging. An axial T1-weighted spin-echo sequence (TR/TE = 516/9) and an axial T2-weighted fast spin-echo sequence (TR/TE = 3200/84, echo train length = 8) with or without fat suppression were used, with a matrix size of 256 × 224, a field of view of 20 × 20 to 22 × 22 cm, a section thickness of 5 mm with an intersection gap of 1 mm, and three signals acquired.

LSDWI studies were conducted within the guidelines of the research committees of our institution. Informed consent was obtained from patients or their authorized representatives. The LSDWI method was described previously (11–14). Neither cardiac gating nor respiratory triggering was used, and no antisusceptibility devices on the neck were used to reduce susceptibility artifacts. LSDWIs were acquired by using the following parameters: TR/TE/NEX = 2376–3124/57.1–70.7/1, field of view of 20 × 20 to 22 × 22 cm, matrix size of 128 × 128 columns, and bandwidth of 3.91 kHz. The effective section thickness was set to 5 mm with an intersection gap of 1 mm. LSDWI images were obtained with two b values, with the maximal b value applied along the three orthogonal directions: one with a low diffusion weighting (b = 5 s/mm^2) and the other with a high (maximum) b factor of 1000 s/mm^2. The imaging time per section was 30–45 seconds, and three to five sections were obtained in the axial plane according to the size of the lesion. Our MR system did not support echo-planar DW imaging with a neurovascular array coil; therefore, echo-planar DW imaging (TR/TE = 9999/69.2, b = 0, 1000 s/mm^2) was performed with a head coil in five patients for comparison with LSDWI.

Spin-echo T1-weighted images (TR/TE = 516/9) and/or gradient-echo images (TR/TE =130/3; flip angle, 80°) were obtained after the intravenous injection of gadopentetate dimeglumine (Magnevist; Japan Schering Co, Osaka, Japan) in all patients except for two patients, who had renal failure.

Imaging Data Analysis

Isotropic diffusion images with b = 1000 s/mm^2 were generated from the three diffusion directions assessed. Trace ADC maps were generated by using the equation Stejskal and Tanner described (17): $S = S_0 e^{-b\mathrm{ADC}}$, where b is the diffusion weighting factor, S is the signal intensity of the diffusion trace for b = maximum, and S_0 is the signal intensity for b = 5 s/mm^2. ADC measurements were obtained from the trace ADC maps by using regions of interest (ROI) placed over the tumors by a neuroradiologist (M.M.). The area of each ROI that was 80 mm^2 or greater was included in the computation. For ROI measurements in the tumors, special care was taken to include the solid-appearing portions of the tumors and to exclude obviously necrotic or cystic regions, as demonstrated in the corresponding T2-weighted and contrast-enhanced MR images. For SCCs, ADC measurements were obtained for only the primary tumor irrespective of metastases to cervical lymph nodes. ADC values were expressed as mean ± standard deviation.

Pathologic Evaluation

Pathologic evaluation was performed for small foci of necrosis in 35 patients with SCC and nine patients with lymphoma by using biopsy specimens. Four patients with SCC and five patients with lymphoma had undergone biopsy at other institutions, and their pathologic specimens were therefore not available for review. A pathologist (H.K.) was asked to assess the pathologic slides of the tumors for small foci of necrosis. When small foci of necrosis were seen in the pathologic specimen, the degree of necrotic foci was graded as mild when the ratio of necrotic areas to tumor areas was less than 0.2 or conspicuous when it corresponding to a ratio of 0.2 or more.

Statistical Methods

The Mann-Whitney U test was used to detect significant differences in mean ADC values between SCC and lymphoma and between well or moderately differentiated SCC and poorly differentiated SCC and also to detect significant differences in the degree of small foci of necrosis of tumors. A P value of less than 0.05 was considered to indicate a statistically significant difference.

Results

ADC Values of SCC and Lymphoma

LSDWI provided diagnostic images (Figs 1–5) and also permitted ADC values to be measured. Apparent necrosis was noted in a single patient with a large SCC, and the ROI measurements were carefully performed to avoid necrotic areas in this patient. Mean

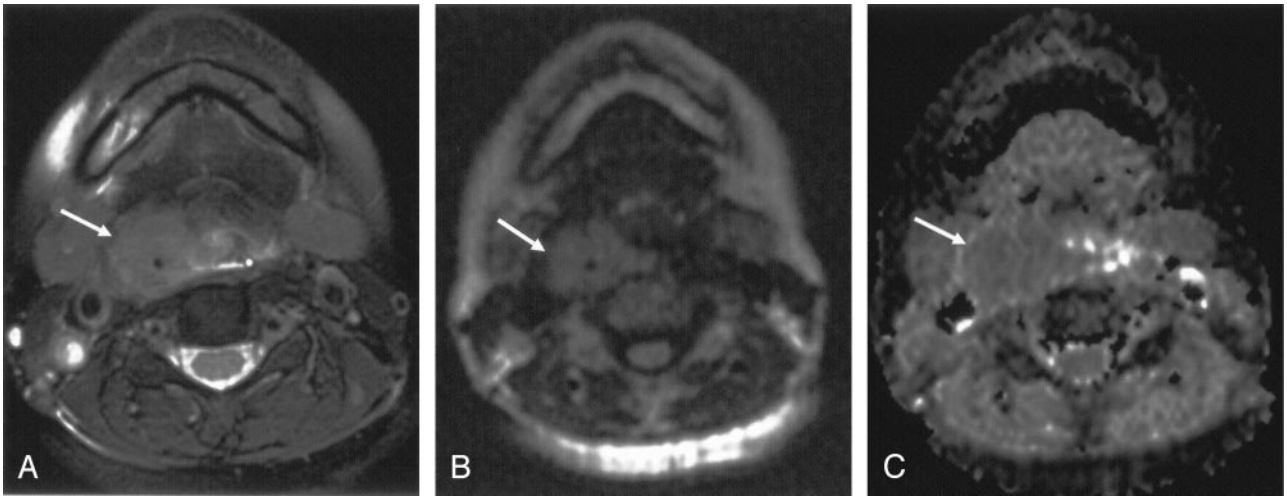

FIG 1. Axial images obtained in a 46-year-old woman with moderately differentiated SCC of the hypopharynx.
A, T2-weighted fat-suppressed MR image shows a mass (*arrow*) in the upper right pyriform sinus.
B, LSDWI obtained with $b = 1000$ s/mm^2 shows a mass (*arrow*). Anatomic details adjacent to the mass are clearly depicted and easily understood.
C, Corresponding ADC map. ADC of the mass (*arrow*) is 0.94×10^{-3} mm^2/s.

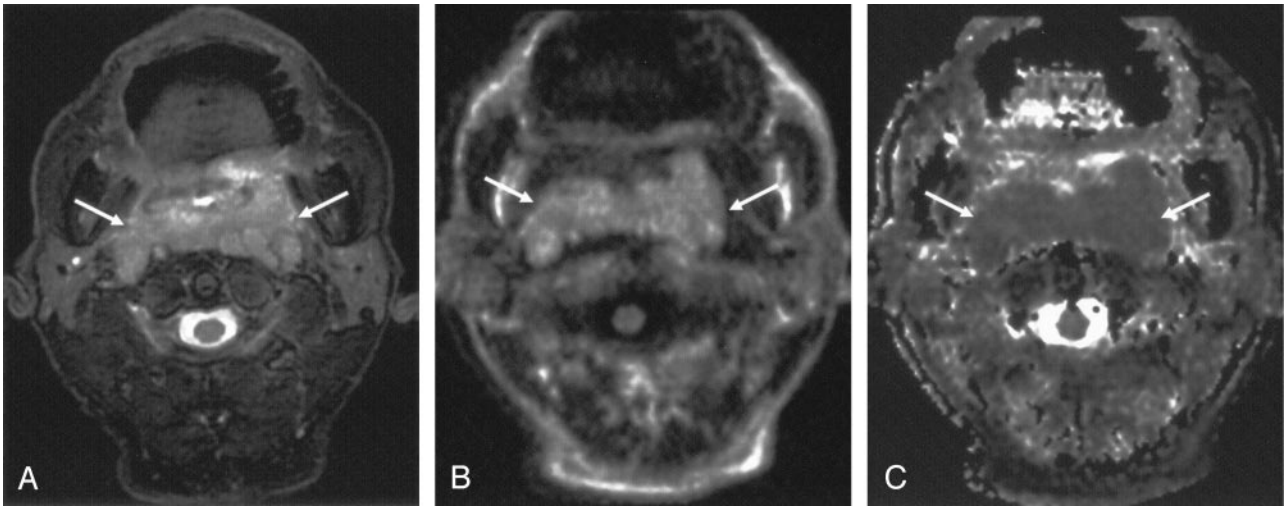

FIG 2. Axial images obtained in a 69-year-old man with diffuse large B-cell lymphoma of the nasopharynx.
A, T2-weighted fat-suppressed MR image shows the mass (*arrows*).
B, LSDWI obtained with $b = 1000$ s/mm^2 shows the mass (*arrows*).
C, Corresponding ADC map. ADC value of the mass (*arrows*) is 0.69×10^{-3} mm^2/s.

ADC values were $0.96 \pm 0.11 \times 10^{-3}$ mm^2/s for SCC and $0.65 \pm 0.09 \times 10^{-3}$ mm^2/s for lymphoma (Fig 6); the difference was significant ($P < .001$). All but one of the patients with lymphoma had ADCs lower than the lowest ADC value (0.76×10^{-3} mm^2/s) observed in those with SCC (Fig 6). When an ADC of 0.76×10^{-3} mm^2/s was used to distinguish between SCC and lymphoma, the accuracy was 98% (52 of 53 lesions).

Mean ADC values for well differentiated ($n = 8$), moderately differentiated ($n = 27$), and poorly differentiated ($n = 4$) SCC were $1.01 \pm 0.08 \times 10^{-3}$, $0.94 \pm 0.11 \times 10^{-3}$, and $0.97 \pm 0.12 \times 10^{-3}$ mm^2/s, respectively (Fig 7). The mean ADC for well or moderately differentiated SCC ($n = 35$) was $0.95 \pm 0.11 \times 10^{-3}$ mm^2/s. ADCs in well or moderately differentiated SCC did not significantly differ from those in poorly differentiated SCC.

Degree of Small Foci of Necrosis in Pathologic Specimens and ADCs

Small foci of necrosis were not seen in the pathologic specimens of 13 (37%) of 35 patients with SCC and of four (44%) of nine patients with lymphoma. Table 2 summarizes the degree of small foci of necrosis and the corresponding ADCs. Although ADC values increased slightly with the degree of small foci of necrosis, the difference was not significant for either type of tumor.

Discussion

The pattern of growth and the clinical symptoms of SCCs and lymphomas are often so characteristic that distinction of the two tumors is possible (18). However, the MR characteristics (e.g., signal intensities

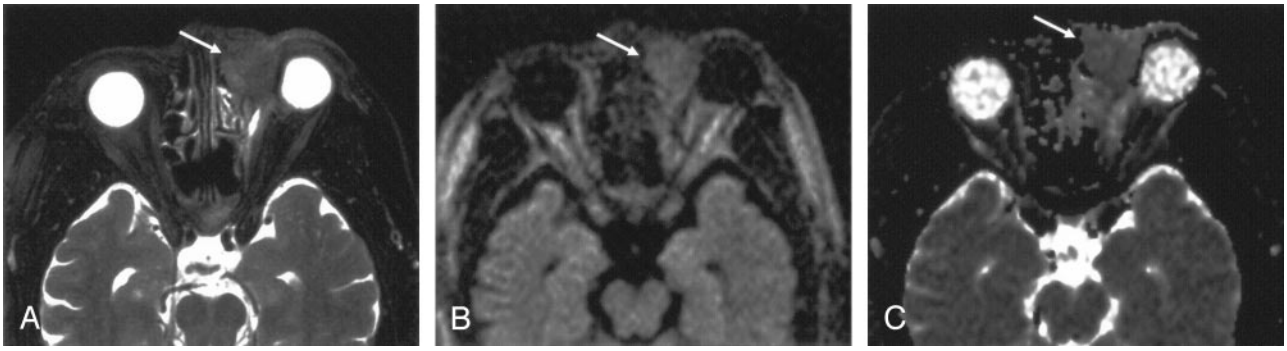

FIG 3. Axial images obtained in a 68-year-old man with moderately differentiated SCC of the left lacrimal sac.
A, T2-weighted fat-suppressed MR image shows the mass (*arrow*).
B, LSDWI obtained with $b = 1000$ s/mm^2 shows the mass (*arrow*).
C, ADC map shows that the signal intensity of the mass (*arrow*) is slightly higher than that of normal brain parenchyma. ADC of the mass is 1.04×10^{-3} mm^2/s.

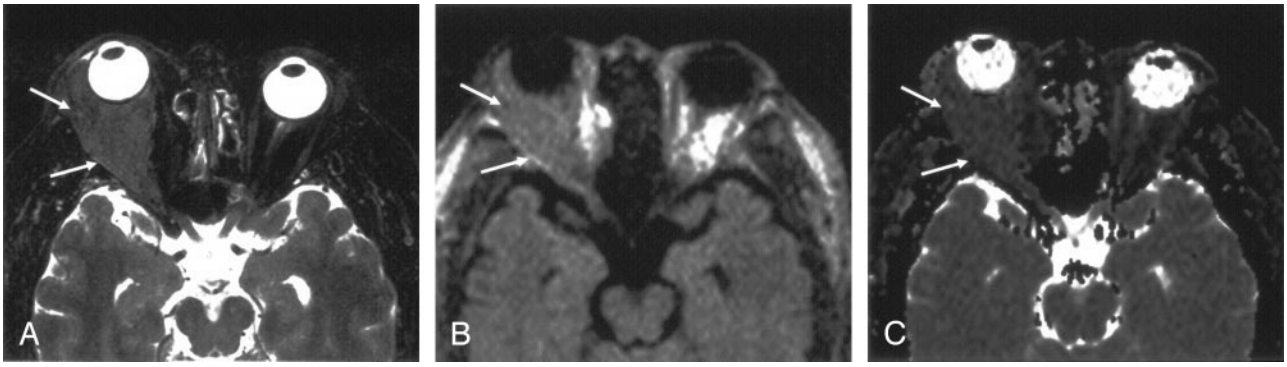

FIG 4. Axial images obtained in a 57-year-old man with marginal zone B-cell lymphoma of the right orbit.
A, T2-weighted fat-suppressed MR image shows the mass (*arrows*).
B, LSDWI obtained with $b = 1000$ s/mm^2 shows the mass (*arrows*).
C, ADC map shows that the signal intensity of the mass (*arrows*) is slightly lower than that of normal brain parenchyma. ADC of the mass is 0.59×10^{-3} mm^2/s.

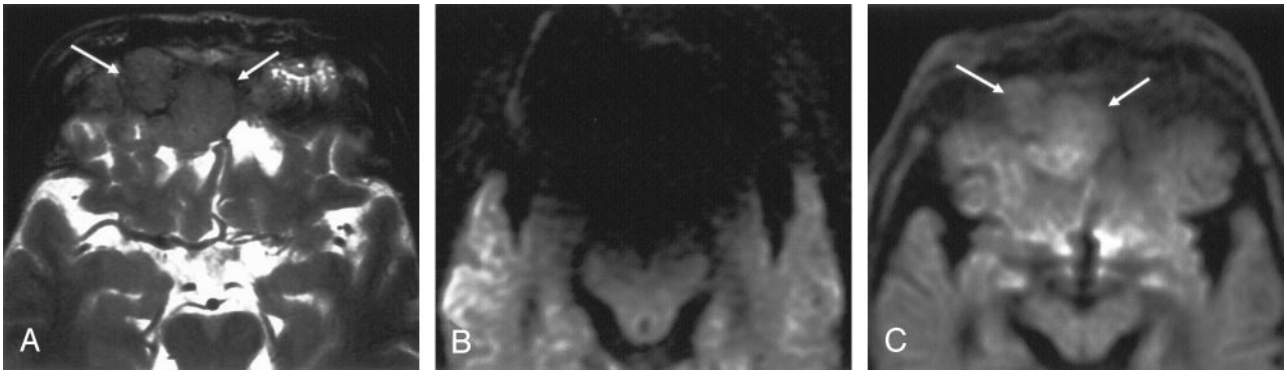

FIG 5. Axial images obtained in a 69-year-old man with moderately differentiated SCC of the right ethmoid sinuses extending intracranially.
A, T2-weighted fat-suppressed MR image shows the mass (*arrows*).
B, Echo-planar DW image obtained with $b = 1000$ s/mm^2 shows significant susceptibility artifacts due to a fixed partial denture, making it impossible to evaluate diffusion.
C, LSDWI obtained with $b = 1000$ s/mm^2 shows the mass (*arrows*) free from susceptibility artifacts.

and contrast enhancement patterns) are sometimes indistinguishable (15). Therefore, distinguishing SCC from lymphoma by using standard anatomic MR imaging techniques can be a challenge.

Our preliminary results showed that LSDWI of the head and neck was feasible and provided diagnostic images without the need for specialized hardware, cardiac gating, or respiratory compensation. In LSDWI, multiple diffusion-weighted, spin-echo column excitations are used to obtain a two-dimensional image (19). This method is relatively insensitive to motion artifacts because the images are constructed column by column, and the acquisition time for an individual column is approximately equal to the TE.

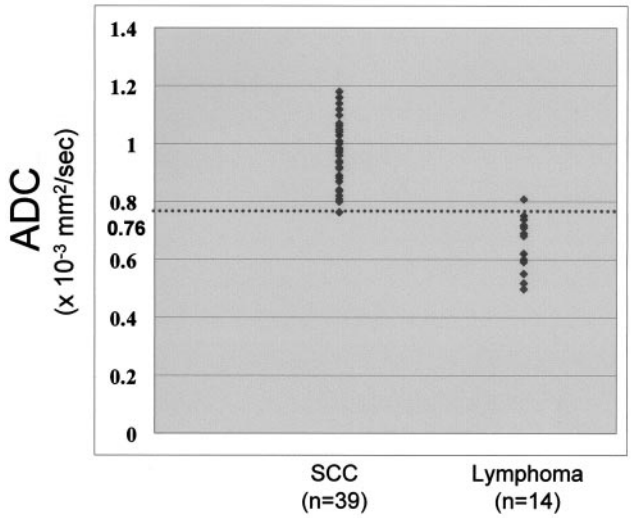

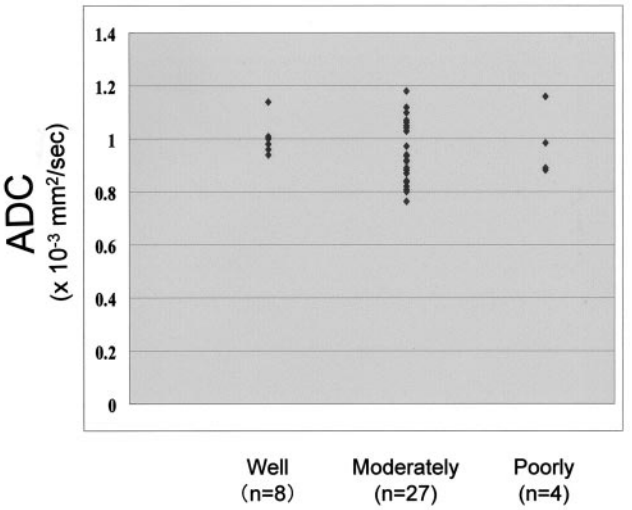

FIG 6. Scatterplot of ADC values in SCC ($n = 39$) and lymphoma ($n = 14$). All but one of the patients with lymphoma had ADCs lower than the lowest ADC (0.76×10^{-3} mm^2/s) in those with SCC. When an ADC of 0.76×10^{-3} mm^2/s (*dotted line*) was used to distinguish between SCC and lymphoma, the accuracy was 98% (52 of 53 lesions).

FIG 7. Scatterplot of ADC values in well ($n = 8$), moderately ($n = 27$), and poorly ($n = 4$) differentiated SCCs. ADCs overlap in the three subtypes of SCC. Well or moderately differentiated SCC ($n = 35$) did not significantly differ from poorly differentiated SCC ($n = 4$).

TABLE 2: ADCs of tumors versus degree of small foci of necrosis in pathologic specimens

	ADC ($\times 10^{-3}$ mm^2/second)		
Lesion	No Necrosis	Mild Necrosis	Conspicuous Necrosis
SCC ($n = 35$)	0.93 ± 0.06 ($n = 13$)	0.96 ± 0.12 ($n = 19$)	1.01 ± 0.09 ($n = 3$)
Lymphoma ($n = 9$)	0.63 ± 0.10 ($n = 4$)	0.73 ± 0.05 ($n = 5$)	Not applicable

Note.—ADC values did not significantly differ according to degree of small foci of necrosis. Data are the mean ± standard deviation.

Patient movement or physiologic pulsatile motion may result in the loss of signal intensity from a column of data, but the rest of the image is unaffected. Unlike single-shot echo-planar DW imaging, LSDWI has minimal susceptibility-related image distortions and loss of signal intensity (11–14, 19); these advantages are essential in DW imaging studies of the head and neck.

In none of our cases did susceptibility artifacts interfere with the evaluation of diagnostic images or ADC values by using the LSDWI technique. Wang et al (7) reported that 16% of their cases had local distortion that affected the lesions on single-shot echo-planar DW images obtained with a *b* factor of 1000 s/mm^2, and their ADC maps were suboptimal because of susceptibility artifacts. They concluded that single-shot echo-planar DW imaging was limited by notable technical limitations related to susceptibility artifacts. First, image distortion along the phase-encoding direction was unavoidable to some degree, and the ADC values in lesions might therefore be inaccurate. Second, it was impossible to measure the ADC values of lesions located adjacent to air, as in the nasopharynx and oropharynx, because of susceptibility artifacts. In addition, we suspect that susceptibility artifacts severely affect single-shot echo-planar DW images, particularly in patients with fixed partial dentures (Fig 5B). We did not compare our LSDWI technique with single-shot echo-planar DW imaging in all cases, but both LSDWI and single-shot echo-planar DW imaging were performed in some cases. With single-shot echo-planar DW imaging, susceptibility artifacts were pronounced (Fig 5B), making it impossible to obtain ADC measurements of the lesions. On the other hand, LSDWI showed no susceptibility artifacts (Fig 5C) and thus permitted us to obtain ADC measurements. The LSDWI technique therefore appears to be more suitable than the echo-planar DW imaging technique for the quantitative assessment of diffusion abnormalities in the head and neck.

Sugahara et al (5) reported that the minimum ADC value has a good correlation with histologic cellularity in gliomas. Guo et al (6) also reported a clear inverse relationship between the ADC value and cellularity of brain tumors, such as lymphomas and high-grade astrocytomas. The ADC value was significantly lower in lymphomas than in high-grade gliomas, whereas cellularity was significantly greater in lymphomas than in high-grade gliomas. Their findings suggest that greater cellularity is associated with more restricted diffusion. Although their data were based on the examination of brain tumors, this hypothesis also appears to be applicable to head and neck tumors.

Our results showed that the ADC value was significantly lower in lymphoma than in SCC. In only one case did the ADC value of a lymphoma overlap

that of SCC. Therefore, ADC values may be useful for distinguishing between these malignant tumors. The difference observed in ADC values may have been due to differences in tumor cellularity. If the above-mentioned hypothesis holds, lymphoma is expected to have greater tumor cellularity than SCC. Although we did not quantitatively analyze tumor cellularity, attenuated aggregates of cells with scanty cytoplasm and an extracellular matrix were commonly observed in our patients with lymphoma, and this finding may explain the lower ADC values obtained for lymphoma than for SCC, as suggested by findings for CNS lymphoma (6).

Apparent necrosis on T2-weighted and contrast-enhanced images was observed in only one of 39 patients with SCC and in none of the patients with lymphoma. On the other hand, pathologic examination revealed that 22 (63%) of 35 patients with SCC had small foci of necrosis of the mild or conspicuous type, whereas five (56%) of nine patients with lymphoma had small foci of necrosis of the mild type. Wang et al (7) speculated that the small foci of necrosis in tumors confirmed by pathologic examination but not identifiable on MR imaging might be the main reason for high ADC values observed in SCC. On the other hand, Lyng et al (20) reported that the fraction of massive necrosis could be correlated with the ADC value but not the fraction of small foci of necrosis because the size of small foci of necrosis may be smaller than the voxel of the MR images. This observation may support our finding that the ADC values of tumors did not significantly differ with degree of small foci of necrosis (Table 2). Although biopsy specimens are small and though they may not accurately reflect the fraction of necrosis in the entire tumor, our results suggest that small foci of necrosis of tumors were not the main reasons for a high ADC value.

Wang et al (7) reported that the ADC values of poorly differentiated carcinoma overlap those of lymphoma, suggesting that ADC values of poorly differentiated carcinoma are lower than those of well or moderately differentiated carcinoma. Sumi et al (10) also reported that ADC values of well or moderately differentiated SCC are higher than those of poorly differentiated SCC and that the ADC values of poorly differentiated SCC approximate those of lymphoma as a result. They ascribed this finding to the hypercellularity of poorly differentiated SCC. On the other hand, our results showed no overlap between lymphoma and poorly differentiated SCC and no significant differences in ADC values according to degree of differentiation in SCC. Why our results are not in agreement with those of previous reports is uncertain. The degree of histopathologic differentiation is not always related to degree of cellularity in malignant tumors. In the histologic grading of SCC, the degree of differentiation is determined by specific findings, such as the keratinization, stratification and atypia of cells, and the degree of cellularity is not particularly significant (21). Therefore, studies in more patients with SCC are needed before we can reach a conclusion on this matter.

The LSDWI technique is robust and applicable to evaluation of ADC values in tumors of the head and neck, where insensitivity to susceptibility artifacts is essential. However, our study had several drawbacks. First, LSDWIs were degraded in five patients who met the inclusion criteria but who were unable to control movement of their head and neck, resulting in their exclusion from this study. Second, we selected *b* factors of 5 and 1000 s/mm^2 to obtain the ADC values. The effect of the perfusion factor may not be eliminated with these *b* factors because transformation between the perfusion and diffusion effects occurs at *b* values in the 100–300 s/mm^2 range (22). Some investigators used relatively high b factors of 500 and 1000 s/mm^2 to avoid the attribution of perfusion factor to the diffusion factor (9, 10). Therefore, the hypervascular portions of SCC might be partly responsible for the increased ADC values observed in our study.

Conclusion

LSDWI is insensitive to susceptibility artifacts and permits the evaluation of ADC values in SCC and lymphoma of the head and neck. ADC values of lymphoma were significantly lower than those of SCC. LSDWI may be useful for distinguishing between SCC and lymphoma.

References

1. Warach S, Chien D, Li W, Ronthal M, Edelman RR. **Fast magnetic resonance diffusion-weighted imaging of acute human stroke.** *Neurology* 1992;42:1717–1723
2. Warach S, Gaa J, Siewert B, et al. **Acute human stroke studied by whole brain echo planar diffusion-weighted magnetic resonance imaging.** *Ann Neurol* 1995;37:231–241
3. Lovblad KO, Laubach HJ, Baird AE, et al. **Clinical experience with diffusion-weighted MR in patients with acute stroke.** *AJNR Am J Neuroradiol* 1998;19:1061–1066
4. Gonzalez RG, Schaefer PW, Buonanno FS, et al. **Diffusion-weighted MR imaging: Diagnostic accuracy in patients imaged within 6 hours of stroke symptom onset.** *Radiology* 1999;210:155–162
5. Sugahara T, Korogi Y, Kochi M, et al. **Usefulness of diffusion-weighted MRI with echo-planar technique in the evaluation of cellularity in gliomas.** *J Magn Reson Imaging* 1999;9:53–60
6. Guo AC, Cummings TJ, Dash RC, Provenzale JM. **Lymphomas and high-grade astrocytomas: comparison of water diffusibility and histologic characteristics.** *Radiology* 2002;224:177–183
7. Wang J, Takashima S, Takayama F, et al. **Head and neck lesions: characterization with diffusion-weighted echo-planar MR imaging.** *Radiology* 2001;220:621–630
8. Yoshino N, Yamada I, Ohbayashi N, et al. **Salivary glands and lesions: evaluation of apparent diffusion coefficients with split-echo diffusion-weighted MR imaging: initial results.** *Radiology* 2002;221:837–842
9. Sumi M, Takagi Y, Uetani M, et al. **Diffusion-weighted echoplanar MR imaging of the salivary glands.** *AJR Am J Roentgenol* 2002;178:959–965
10. Sumi M, Sakihama N, Sumi T, et al. **Discrimination of metastatic cervical lymph nodes with diffusion-weighted MR imaging in patients with head and neck cancer.** *AJNR Am J Neuroradiol* 2003;24:1627–1634
11. Maier SE, Gudbjartsson H, Patz S, et al. **Line scan diffusion imaging: characterization in healthy subjects and stroke patients.** *AJR Am J Roentgenol* 1998;171:85–93
12. Maeda M, Sakuma H, Maier SE, Takeda K. **Quantitative assess-**

ment of diffusion abnormalities in benign and malignant vertebral compression fractures by line scan diffusion-weighted imaging. *AJR Am J Roentgenol* 2003;181:1203–1209
13. Nagata M, Maeda M, Tsukahara H, Maier SE, Takeda K. **Brain stem hypertensive encephalopathy evaluated by line scan diffusion-weighted imaging.** *AJNR Am J Neuroradiol* 2004;25:803–806
14. Maeda M, Shimono T, Tsukahara H, Maier SE, Takeda K. **Acute bilateral medial medullary infarction: a unique "heart appearance" sign by diffusion-weighted imaging.** *Eur Neurol* 2004;51:236–237
15. Grossman RI, Yousem DM. *Neuroradiology: The Requisites.* St. Louis: Mosby;381–388
16. King AD, Yuen EHY, Lei KIK, Ahuja AT, van Hasselt A. **Non-Hodgkin lymphoma of the larynx: CT and MR imaging findings.** *AJNR Am J Neuroradiol* 2004;25:12–15
17. Stejskal EO, Tanner JE. **Spin diffusion measurements: spin echoes in the presence of a time-dependent field gradient.** *J Chem Phys* 1965;42:288–292
18. King AD, Lei KIK, Richards PS, Ahuja AT. **Non-Hodgkin's lymphoma of the nasopharynx: CT and MR imaging.** *Clin Radiol* 2003;58:621–625
19. Gudbjartsson H, Maier SE, Mulkern RV, et al. **Line scan diffusion imaging.** *Magn Reson Med* 1996;36:509–519
20. Lyng H, Haraldseth O, Rofstad EK. **Measurement of cell density and necrotic fraction in human melanoma xenografts by diffusion weighted magnetic resonance imaging.** *Magn Reson Med* 2000;43:828–836
21. Barry JD, Sharkey FE. **Morphometric grading of squamous cell carcinoma.** *Histopathology* 1986;10:1143–1152
22. Le Bihan D. **Molecular diffusion nuclear magnetic resonance imaging.** *Magn Reson Q* 1991;7:1–30